RESEARCH ARTICLE

Unraveling Impact of Critical Sensor Density on Occlusion Coverage of Partial Targets for Directional Sensor Networks

ZHIMIN LIU[ID]**1, ZUOQING CAO**[ID]**2, SHUKUN LIU**[ID]**3, (Member, IEEE), AND PINIAL KHAN BUTT**[ID]**4**

[1]School of Computer Science, Hunan First Normal University, Changsha 410002, China
[2]School of Mapping and Geography, Hunan Engineering Vocational and Technical College, Changsha 410151, China
[3]School of Computer Science and Technology, Hunan Women's University, Changsha 410004, China
[4]Information Technology Center, Sindh Agricultural University, Tondo Jam 70060, Pakistan

Corresponding author: Zuoqing Cao (clkingt@163.com)

ABSTRACT Coverage is a prominent indicator for measuring the quality of service in directional sensor networks. From the perspective of energy and deployment costs, full coverage may be expensive or unrealistic, partial coverage can operate more energy-efficient by scheduling working status of sensors. In certain practical application scenarios, irregular obstacles like trees, mountains, buildings, and vehicles, which have adverse influence on QoC, often exist in the field of interest (FoI). Meanwhile, due to sensors may fall near the border of the FoI, it also has effect on the coverage contribution. In this paper, we assume that sensors are randomly deployed in a square FoI with irregular shape obstacles existence, and introduce the concept of occlusion coverage of partial targets. Afterwards, we take the border effects into account and derive the critical sensor density for achieving an expected coverage ratio with a high probability. Finally, we conduct a series of simulation experiments to verify the accuracy between simulation results and numerical results, and take analysis of mean absolute error between them. The results show that our method has good performance on estimating critical sensor density.

INDEX TERMS Directional sensor networks, target coverage, critical sensor density, irregular obstacles, border effects.

I. INTRODUCTION

As a derivative of wireless sensor networks (WSNs), a typical directional sensor network (DSN) is composed of several battery-powered directional sensors (sensors) which own sector-disk sensing regions, it has witnessed a vigorous development. Specially, DSN monitoring some targets located in a field of Interest (FoI) usually encountered in many applications such as smart cities, smart industrial monitoring, smart agriculture, wildlife protection and underwater monitoring [1], [2], [3], [4], [5]. In general, target coverage is also a prominent metric for measuring the quality of monitoring of DSN, which reflects how well the targets in the FoI are monitored. Any target in the FoI can be detected if it is located in the sensing region of at least one sensor, we call it full target coverage, its coverage ratio is approximate to 1.

The associate editor coordinating the review of this manuscript and approving it for publication was Rakesh Matam[ID].

In certain applications like wildlife protection and underwater monitoring, full target coverage may be unrealistic or costly. The partial target coverage problem refers to ensure that a part of targets should be covered to achieve an expected quality of coverage (QoC). In this case, DSN can operate more energy-efficient by scheduling redundant sensors to sleep or not sleep so that the network service lifetime can be prolonged. Typically, the coverage ratio of partial targets must be less than a predefined threshold.

In DSN, the random deployment strategy is favored in such scenario where the FoI is hostile or unreachable. In this case, the sensors are typically deployed in random by aircraft rather than manually deterministic deployment so that the QoC may not be predetermined, and it also be unrealistic to achieve full target coverage without a large density of sensors. Meanwhile, 3D irregular shape obstacles like trees, mountains, buildings, vehicles and walls often exist in the FoI, the 3D visual occlusion may be formed which would
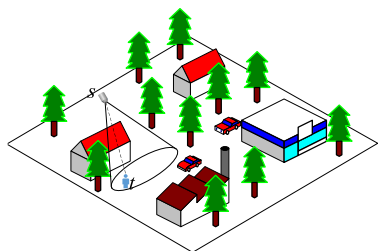
FIGURE 1. Illustration of 3D irregular shape obstacle and its visual occlusion.
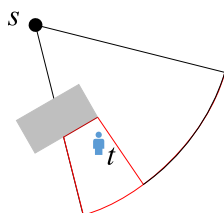

FIGURE 2. Illustration of 2D projection obstacle and its visual occlusion on plane, gray rectangle is the 2D irregular obstacle and dot line region is the 2D visual occlusion.

cause a negative impact on the QoC, as shown in Fig.1. Meanwhile, aiming to obtain the 2D irregular shape obstacle and its 2D visual occlusion, we project the 3D irregular shape obstacle and 3D visual occlusion onto 2D plane, respectively, as illustrated in Fig.2. Since the randomness of deployment of sensors and the obstacles existence result in that the estimation of critical sensor density becomes an important issue to be addressed in DSN. In this paper, we derive the CSD for achieving an expected coverage ratio of partial targets in a square FoI with irregular shape obstacles existence.

Intuitively, if a sensor lies near the border of the FoI, its effective sensing region could be less than its sensing region, which leads to border effects. It is obvious that the estimated CSD for a pre-defined coverage ratio of targets without considering border effects would be less than the actual value. In this paper, we address the problem: *by considering a square FoI where irregular shape obstacles are scattered at random and the border effects, what is the CSD for achieving an expected coverage ratio of partial targets with a high probability*. The results also can be applied to other regular shape obstacles like rectangle, circle, etc. To the best of our knowledge, there is no relevant work on this issue.

The main contributions of this paper are summarized as follows

- We present 2D projection model of 3D irregular shape obstacle, and introduce the concept of occlusion coverage of target.
- We estimate the expected value of effective possible sensing region with considering border effects, and introduce the expected occlusion zone between target and sensor. Then, we derive the expression of CSD required to achieve an expected occlusion coverage ratio of targets with a high probability.
- We present the simulation results to take analysis of the influence of border effects and obstacles on CSD.

The rest of this paper is organized as follows: Section II briefly introduce the related works. In Section III, we present system model and definitions. The expected value of the effective possible sensing region with considering border effects is derived in Section IV. Section V presents the expression of CSD for an expected occlusion coverage ratio of targets. A series of simulation experiments are conducted to verify the accuracy of numerical results in Section VI. Finally, Section VII is the conclusion and the possible future works are presented.

II. RELATED WORKS

Currently, the coverage issue has attracted widespread attention from academia and industry. In this section, we briefly review important contributions in the literatures on coverage and critical sensor density estimation.

In conventional WSNs, Ammari and Das [6] proposed an integrated-concentric-sphere model to address coverage and connectivity in 3D WSNs, authors first derived λ^{cov} and λ^{con} to ensure that coverage percolation and connectivity percolation almost surely occur, respectively. Then, a critical density $\lambda^{cov-con}$ is presented to ensure that coverage and connectivity percolation simultaneously occur with a high probability. The authors in [7] assumed that the FoI is a convex polygon-shaped, and taken the border effects into account. Then, they derived the critical sensor density for achieving an expected coverage ratio. Wang et al. [8] studied the critical sensor density issue of achieving full coverage in WSNs, and derived the upper and lower bound for the average vacancy as critical sensor density to achieve full coverage. Yoon and Kim [9] derived the upper and lower bounds on the coverage of a 2D deployment of static sensors. In [10], authors assumed that the sensors, which may not have the same sensing radius, are deployed at random uniformly in a three-dimensional FoI, and derived the critical condition for the expected level of coverage of the FoI using a probabilistic model. Saha et al. [11] proposed a fast and nearly-accurate method of estimating the area covered by a set of n identical sensors randomly deployed in a 2D FoI.

Due to the sensing region of sensor in DSNs is a sector-disk region, the existing works in WSNs cannot be directly applied to solve such issues in DSNs. Karakaya and Qi [12] taken the radius and the visual occlusion of target into account in crowded targets environment, authors derived the closed-form solution for the estimation of the visual coverage probability based on certainty-based target detection model, but they did not consider that the irregular shape obstacles (such as tree, building, mountain and wall etc) may be exist between the sensor and the target. Literatures [13] and [14] proposed a critical sensor density approach to ensure coverage and connectivity for field-of-view angles between 0 and π by using continuum percolation. However, visual occlusion and border effects issues were not considered. Attar et al. [15] also studied the coverage estimation issue in visual sensor networks, and validated the proposed mathematical solution. In [16],
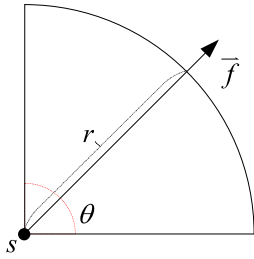
FIGURE 3. Illustration of sensing model.

authors first proposed full-view coverage model, and derived a necessary and sufficient condition on sensor density for complete full-view coverage ratio. Following that, Wang and Cao [17] also analyzed that condition to achieve complete full-view coverage ratio, besides, they introduce verification problems of weak/strong full-view barrier and their detection methods. Aiming to mobile camera sensor networks, authors in literature [18] taken the initiative to address the critical condition to achieve asymptotic full-view coverage in mobile DSN, and proposed equivalent sensing radius (ESR) to unravel the critical requirement for asymptotic full-view coverage by ignoring border effects. Liu and Jiang [19] assumed that the sensors are randomly deployed in an irregular bounded region, and derived the sensor parameter estimation model for the expected full-view coverage ratio with a high probability. Yu et al. [20] proposed a novel local face-view coverage model, and derived coverage estimation model under deterministic deployment. Kang et al. [21] proposed an approach to compute critical density to ensure entire coverage and full connectivity.

Most literatures do not take the border effects and irregular shape obstacles into account. Although some of works consider the target radius and target visual occlusion in crowded targets environment, but they assume that none of obstacles exist in the FoI.

III. MODELS AND PROBLEM DEFINITION
In this section, we present the sensing model of directional sensor (sensor), 2D projection model of 3D irregular obstacle, system model and relevant definitions.

A. SENSING MODEL OF SENSOR
A binary sector model is commonly used in many literatures [13], [14], [15], [16], [17], [18], [19]. In general, the sensing model is represented as a 4-tuple $< s, r, \theta, \vec{f} >$, where s denotes a sensor and its position, r denotes its sensing radius, $\vec{f}$ denotes its working direction, θ denotes the field of view (FoV) angle of a sensor. As illustrated in Fig.3, it is obvious that the sensor's sensing region is a sector-disk.

B. 2D PROJECTION MODEL OF OBSTACLE
We take the exact geometric shape of an obstacle into account. The 2D projection of a 3D irregular shape obstacle on a plane is usually an irregular polygon which can be categorized as convex polygon and concave polygon. In literature [22],
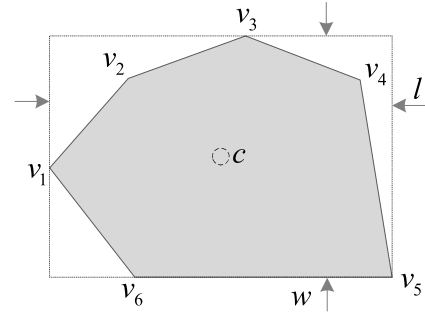

FIGURE 4. Illustration of 2D projection model of an obstacle.

authors proved that any concave polygon can be composed by multiple convex polygons. Therefore, we can conclude that the 2D projection of an obstacle consists of one or more convex polygon.

To simplify the issue we studied, as illustrated in Fig.4, the 2D projection model of an obstacle is represented as a 6-tuple $< rec, c, \mathbf{v}, l, w, \beta >$, where rec denotes the convex polygon's minimum bounding rectangle which can be found by using algorithm in literature [23], c is the center point of rec, we also let it denote the obstacle and the convex polygon, l and w respectively denote the length and width of rec, $\mathbf{v} = \{v_j\}_{j=1\cdots J}$ denotes all vertices of the convex polygon c, β represents the rotation angle of the straight line formed by these two vertices with maximum Euler distance.

C. SYSTEM MODEL
In this paper, the FoI, where is hostile or unreachable, is assumed to be a 2D square area Ω with edge length of L. Thus, we often adopt a random deployment strategy, which inevitably leads to border effects. Besides, the 2D projection convex polygon of a 3D irregular shape obstacle lies inside the FoI would lead to an adverse impact on the QoC. Unlike the previous literatures, we simultaneously consider the border effects and the heterogeneous obstacles.

As illustrated in Fig.5, we assume that n homogeneous sensors $s_1, s_2, \cdots, s_n$ are randomly and uniformly deployed in the FoI, and independent of each other. Moreover, m targets $t_1, t_2, \cdots, t_m$ are randomly distributed in the FoI, we ignore the radius of target. According to the convex polygon c introduced in above section, we divide the obstacles randomly and independently located in the FoI into u groups $g_1, g_2, \cdots, g_u$, it is obvious that the corresponding convex polygons have the same grouping. Let ϖ_i be the number of obstacles in group g_i. Clearly, the total number of obstacles is represented as $\varpi = \varpi_1 + \varpi_2 + \cdots + \varpi_u$. each obstacle in group g_i has identical convex polygon c_i, but either $c_i \neq c_j$ will hold if $i \neq j$. On the basis of the system model studied in this paper, we use convex polygon to denote any obstacle projected onto 2D plane.

D. DEFINITIONS
To better evaluate the sensing performance of a sensor in DSN, we give the following definitions.
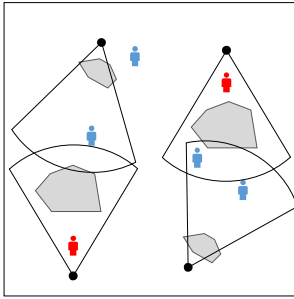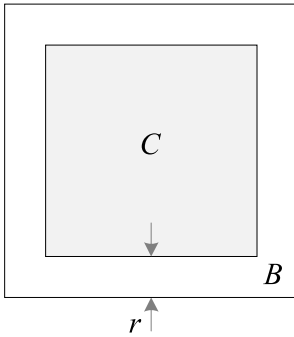
FIGURE 5. Illustration of system model.

FIGURE 6. Illustration of border zone and center zone.
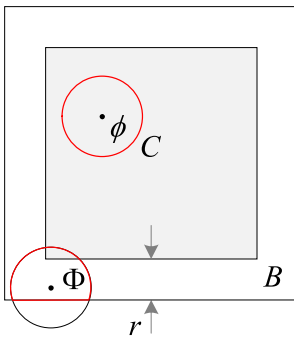

FIGURE 7. Illustration of possible sensing region and effective possible sensing region.

1) BORDER ZONE AND CENTER ZONE

As illustrated in Fig.6, It can be seen that the FoI can be categorized by two disjoint regions: the border zone B, and the center zone C. It is easy to infer that the border zone is a strip with width of r which denotes the sensing radius. Then, we get $C = \Omega - B$.

2) POSSIBLE SENSING REGION (PSR)

For a sensor s, the circle region centered at it with radius r is called as the possible sensing region denoted as ϕ, as shown in Fig.7. Clearly, its area can be expressed as $|\phi| \doteq \pi r^2$.

3) EFFECTIVE POSSIBLE SENSING REGION (EPSR)

From Fig.7, we conclude that the intersection of the PSR and the FoI is called effective possible sensing region which is denoted as $\Phi = \phi \cap \Omega$. Obviously, when a sensor lies inside the center zone C, its EPSR is the PSR itself. However, if the
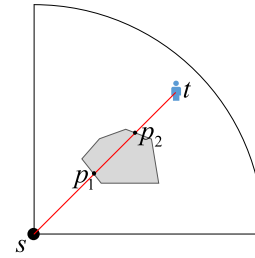

FIGURE 8. Illustration of a target being occluded by an obstacle, p_1 and p_2 are the two intersections of line segment st and edges of 2D projection convex polygon of the obstacle.

sensor lies inside the border zone B, its EPSR is not greater than PSR, we get $|\Phi| \leq \pi r^2$.

4) OCCLUSION COVERAGE

As illustrated in Fig.8, for a target t, if the target is covered by at least one sensor s and the line segment st is not intersect with the edges of the convex polygon of any obstacle, we conclude that the target achieves occlusion coverage which can be verified by checking the following three mathematical conditions.

- $dist(s, t) \leq r$.
- $\alpha(\vec{f}, \vec{st}) \leq \theta/2$
- For any convex polygon c_i, if $\exists p_j(x_{ij}, y_{ij}) = st \cap edgeof(c_i)$, and $(x^s - x_{ij})(x^t - x_{ij}) > 0$. Where $j = 1, 2$, and x^s, x^t represent the X-axis coordinates of the sensor s and the target t, respectively.

The condition 1 and condition 2 indicate that the target t must be located inside the sensing region of the sensor s. The condition 3 indicates that the line segment st is not intersect with the edges of any convex polygon c_i.

E. MAIN SYMBOLS

In order to describe the problem more clearly, the main symbols used in this paper are summarized in Table 1.

IV. ESTIMATION OF EXPECTED EPSR WITH CONSIDERING BORDER EFFECTS

In this section, for a sensor s lies in the FoI, we start with estimating the expected value of its EPSR.

As we mentioned in **Definition 3**, it is obvious that the expected EPSR depends on the location of the sensor s. Let $E[\Phi_c]$ denote the expected EPSR of the sensor lies inside center zone C, and $E[\Phi_b]$ denote that of it lies inside the border zone B, we obtain $E[\Phi_c] = \pi r^2$, but $E[\Phi_b]$ is unknown. Due to the sensor randomly lies in either C or B, the expected EPSR of it in the FoI, denoted as $E[\Phi]$, can be given by

$$E[\Phi] = \frac{|C|}{|\Omega|}E[\Phi_c] + \frac{|B|}{|\Omega|}E[\Phi_b] \qquad (1)$$

where $|\Omega|$ denotes the area of the FoI. In the rest of this section, we derive $E[\Phi_b]$ by approximating the border zone B to be an equivalent rectangle zone. Specially, if we do

TABLE 1. Description of symbols.

| Notation	Description
Ω	Square FoI
L	Length of FoI
$\|\Omega\|$	Area of FoI
m	Number of Targets
u	Number of Groups of Obstacles
g_i	The ith group of obstacles, $1 \leq i \leq u$
ϖ_i	Number of obstacles in g_i
μ_i	Density of Obstacles Belong to g_i
$\varpi = \sum_{i=1}^{u} \varpi_i$	Total number of Obstacles
n	Number of Sensors
r	Sensing Radius
θ	FoV Angle
ρ	Critical Sensor Density
ϕ	Possible Sensing Region
Φ	Effective Possible Sensing Region
C	Center Zone
B	Border Zone
Φ_b	EPSR in Border Zone
Φ_c	EPSR in Center Zone
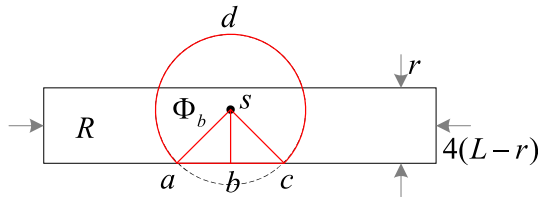
FIGURE 9. Illustration of the rectangle zone R approximating to the border zone B.

not take the border effects into account, we easily obtain $E[\Phi_b] = E[\Phi_c] = \pi r^2$.

Intuitively, if the sensor s lies inside the border zone B, its PSR will intersect with the external region of the FoI, resulting in border effects. Then, we consider the border effects and derive the formula of $E[\Phi_b]$. Before derivation, we have the following lemma.

Lemma 1: The area of the border zone B is equal to the area of a rectangle zone R with a length of $4(L - r)$ and a width of r.

Proof: From Fig.3, clearly, we obtain $|\Omega| = L^2$ and $|C| = L^2 - 4Lr - 4r^2$. Thus, the area of the border zone B can be calculated by $|B| = |\Omega| - |C| = 4(L - r)r$, this value is exactly equal to the area of the rectangle zone R in **Lemma 1**. The **Lemma 1** is proved.

According to **Lemma 1**, the rectangle zone R can be used to approximate the border zone B. Thus if the sensor s lies inside the border zone, it can be approximated that it lies inside the rectangle zone. From Fig.9, let (x, y) be the coordinates of the sensor in the rectangle zone, thus, the area of the EPSR can be calculated by the following formula

$$|\Phi_b| = \pi r^2 - \left(S_{\widehat{sabc}} - S_{\triangle sac} \right)$$
$$= \frac{1}{2}r^2 \left(2\pi - 2\arccos\left(\frac{y}{r}\right) + \sin\left(2\arccos\left(\frac{y}{r}\right)\right)\right)$$

(2)

Therefore, the expected EPSR of the sensor s lies inside border zone B can be simply integrated $|\Phi_b|$ over R, its value can be approximately given by

$$E[\Phi_b] = \frac{\int \int |\Phi_b| dR}{|R|}$$
$$= \frac{\int_0^r \int_0^{4(L-r)} |\Phi_b| dy dx}{4r(L - r)}$$

(3)

By combining Equations (1)(2)(3), we obtain that the expected EPSR of the sensor s in the FoI can be expressed as

$$E[\Phi] = \frac{(L^2 - 4Lr - 4r^2)\pi r^2 + \int_0^r \int_0^{4(L-r)} |\Phi_b| dy dx}{L^2}$$

(4)

V. CRITICAL SENSOR DENSITY

In the previous section, we estimated the expected EPSR of a sensor lies anywhere in the FoI. In this section, we start with the analysis of partial target coverage with obstacles existence, and derive the critical sensor density for an expected target coverage ratio with a high probability. We first have the following lemma.

Lemma 2: Given any subarea A' of area A and N number of random points in area A. Let $X_{A'}$ be a random variable representing the number of points in the subarea A'. The probability of the event $\{X_{A'} = k\}$ is expressed as

$$P(X_{A'} = k) = e^{-\lambda |A'|} \frac{(\lambda |A'|)^k}{k!}$$

(5)

where $k \geq 0$, $|A'|$ is the area of A' and $\lambda = \frac{N}{|A|}$ is the point density per unit area.

Proof: Let H be the random variable representing if a point lies in subarea A' or not, its value is 1 or 0. We get the probability of event $\{H = 1\}$ is calculated by $P(H = 1) = \frac{|A'|}{|A|}$. Event $\{X_{A'} = k\}$ follows Binomial Distribution, its probability can be expressed as

$$P(X_{A'} = k) = \binom{N}{k} (P(H = 1))^k (1 - P(H = 1))^{N-k}$$

Let $\lambda = \frac{N}{|A|}$, we get

$$\lim_{N \to \infty} P(X_{A'} = k)$$
$$= \lim_{N \to \infty} \binom{N}{k} (P(H = 1))^k (1 - P(H = 1))^{N-k}$$
$$= \lim_{N \to \infty} \frac{N!}{(N-k)!k!} \left(\frac{|A'|}{|A|}\right)^k \left(1 - \frac{|A'|}{|A|}\right)^{N-k}$$
$$= \lim_{N \to \infty} \frac{N!}{(N-k)!k!} \left(\frac{\lambda |A'|}{N}\right)^k \left(1 - \frac{\lambda |A'|}{N}\right)^N \left(1 - \frac{\lambda |A'|}{N}\right)^{-k}$$
$$= e^{-\lambda |A'|} \frac{(\lambda |A'|)^k}{k!}$$
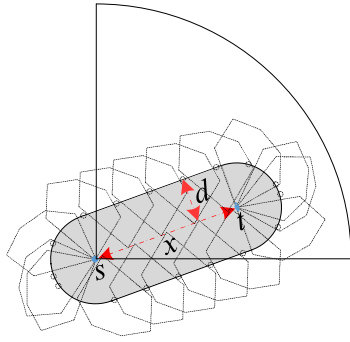
The **Lemma 2** is proved.

FIGURE 10. Illustration of expected occlusion zone, gray region denotes the expected occlusion zone.

A. PROBABILITY OF NO VISUAL OCCLUSION BETWEEN TARGET AND SENSOR

According to the system model we studied, ϖ number of irregular obstacles, which classified into u groups, are randomly located in the FoI, and independent of each other. These obstacles may generate visual occlusion exist between a target t and a sensor s. In this section, we assume that the target t lies inside the sensing region of the sensor s. Let $x \in [0, r]$ be the Euler distance between them. Then we randomly take an obstacle in group g_i into account, and derive the probability of the event that there is no visual occlusion between the target and the sensor.

When the minimum bound rectangle rec_i of the obstacle is tangent to the line segment st, let d_i be the vertical distance from the center point of rec_i to the line segment st, we can obtain $d_i \in \left[\frac{w_i}{2}, \frac{\sqrt{l_i^2 + w_i^2}}{2} \right]$. In this situation, an occlusion zone denoted is formed. Due to the rotation angle β_i of the obstacle is randomly and uniformly distributed, we know that the d_i also follows unform random distribution, and its expected value $\overline{d_i} = \frac{w_i + \sqrt{l_i^2 + w_i^2}}{4}$. Thus the expected occlusion zone denoted as A_i' can be approximately calculated by $|A_i'| = \pi \overline{d_i}^2 + 2\overline{d_i}x$, as illustrated Fig.10. Each obstacle in the same group forms identical expected occlusion zone, but either $A_i' \neq A_j'$ will hold if $i \neq j$.

In order to make the line segment st to be not occluded by any obstacle in group g_i, it must be satisfied that there is no such obstacle lies inside the expected occlusion zone A_i'. Let $X_{A_i'}$ be the random variable representing the number of group g_i obstacles located inside the expected occlusion zone A_i'. Base on the **Lemma 2**, the probability of the event $X_{A_i'} = 0$ is approximately expressed as

$$P(X_{A_i'} = 0) = e^{-\mu_i |A_i'|} \frac{(\lambda |A_i'|)^0}{0!}$$
$$= e^{-\mu_i \left(\pi \overline{d_i}^2 + 2\overline{d_i}x \right)} \qquad (6)$$

where $\mu_i = \frac{\varpi_i}{|\Omega|}$ is the density of group g_i obstacles per unit area.

Let $X = \sum_{i=1}^{u} X_{A_i'}$ be the random variable representing the number of obstacles in all groups $g_1, g_2, \cdots, g_u$

located in their corresponding expected occlusion zones $A_1', A_2', \cdots, A_u'$. Due to these obstacles are independent of each other and the value of random variable $X_{A_i'}$ must not be less than zero, we know that the probability of the event $\{X = 0\}$ is expressed as

$$P(X = 0) = P\left(\sum_{i=1}^{u} X_{A_i'} = 0 \right)$$
$$= \bigcap_{i=1}^{u} P\left(X_{A_i'} = 0 \right)$$
$$= e^{\sum_{i=1}^{u} \mu_i \left(\pi \overline{d_i}^2 + 2\overline{d_i}x \right)} \qquad (7)$$

Due to $P(X = 0)$ is the function of $x \in [0, r]$ which is a random value about distance from the sensor to the target, we can get that the expected value of $P(X = 0)$ is often used to describe probability of the event $\{X = 0\}$ more accurately. Let $E[X = 0]$ be the expected value of that probability. Clearly, $E[X = 0]$ can be obtained by simply integrating $P(X = 0)$ over $[0, r]$, it can be expressed as

$$E[X = 0] = \frac{\int_0^r P(X = 0)dx}{r}$$
$$= \frac{\int_0^r e^{\sum_{i=1}^{u} \mu_i \left(\pi \overline{d_i}^2 + 2\overline{d_i}x \right)} dx}{r} \qquad (8)$$

B. PROBABILITY OF TARGET TO BE COVERED WITH CONSIDERING VISUAL OCCLUSION

In the previous derivation, we assume that the target t is always located inside the sensing region of the sensor s, but do not consider how to estimate the probability of the event that at least one sensor covers the target t. In this section, we take analysis of this issue with considering visual occlusion.

Let Y be the random variable representing if the target t is exactly covered by one sensor s or not, its values is 1 or 0. Event $\{Y = 1\}$ represents that the target t lies inside the sensing region of one sensor. We assume that all sensors follow a uniform distribution, it is easy to get that the probability of the event $\{Y = 1\}$ is expressed as

$$P(Y = 1) = \frac{E[\Phi]}{|\Omega|} \frac{\theta}{2\pi} \qquad (9)$$

where $E[\Phi]$ is given by Equation (4), $\frac{E[\Phi]}{|\Omega|}$ represents that the probability of the target lies inside the expected EPSR of the sensor, $\frac{\theta}{2\pi}$ represents that the probability of the target is located within the FoV angle of the sensor.

Let $\mathcal{Z}$ be an event to represent that the target t is exactly covered by one sensor s and the line segment st is not occluded by any obstacle. According to the previous derivations, the probability of this event can be expressed as

$$P(\mathcal{Z}) = P(Y = 1)E(X = 0)$$
$$= \frac{E[\Phi]}{|\Omega|} \frac{\theta}{2\pi} E(X = 0)$$
$$= \frac{E[\Phi]}{|\Omega|} \frac{\theta}{2\pi} \frac{\int_0^r e^{\sum_{i=1}^{u} \mu_i \left(\pi \overline{d_i}^2 + 2\overline{d_i}x \right)} dx}{r} \qquad (10)$$

Then, we conduct the above-mentioned random experiment n times (n also denotes the number of sensors), and let F be a random variable representing the number of sensors exactly occlusion covering the target t. It is obvious that the event $\{F = 0\}$ represents that the event $\mathcal{Z}$ is not happened in each experiment, we get that its probability can be expressed as

$$P(F = 0) = (1 - P(\mathcal{Z}))^n$$

$$= \left(1 - \frac{E[\Phi]}{|\Omega|} \frac{\theta}{2\pi} \frac{\int_0^r e^{\sum_{i=1}^u \mu_i \left(\pi \overline{d_i}^2 + 2\overline{d_i}x \right)} dx}{r} \right)^n$$

(11)

Base on the knowledge of probability, the probability of the event $\{F \geq 1\}$ denoting that at least one sensor occlusion covers the target t is given by

$$P(F \geq 1) = 1 - P(F = 0)$$

$$= 1 - \left(1 - \frac{E[\Phi]}{|\Omega|} \frac{\theta}{2\pi} \frac{\int_0^r e^{\sum_{i=1}^u \mu_i \left(\pi \overline{d_i}^2 + 2\overline{d_i}x \right)} dx}{r} \right)^n$$

(12)

The expected value of the occlusion coverage ratio of targets with considering visual occlusion, denoted by $E[\mathcal{T}]$, is the ratio of the number of the targets t occlusion covered by at least one sensor to the total targets. Therefore

$$E[\mathcal{T}] = \frac{mP(F \geq 1)}{m}$$

$$= P(F \geq 1)$$

(13)

where m denotes the number of targets located in the FoI.

C. CRITICAL SENSOR DENSITY WITH CONSIDERING VISUAL OCCLUSION

In this section, we derive the critical sensor density for achieving an expected occlusion coverage ratio of partial targets with a high probability.

Theorem 1: Given a square FoI Ω where sensors, targets and irregular shape obstacles are uniformly scattered, and an expected value of occlusion coverage ratio $E[\mathcal{T}]$, where $E[\mathcal{T}] \in [0, 1]$. The critical sensor density ρ which is needed to ensure $E[\mathcal{T}]$ with a high probability is expressed as

$$\rho = \frac{ln(1 - E[\mathcal{T}])}{|\Omega| ln \left(1 - \frac{E[\Phi]}{|\Omega|} \frac{\theta}{2\pi} \frac{\int_0^r e^{\sum_{i=1}^u \mu_i \left(\pi \overline{d_i}^2 + 2\overline{d_i}x \right)} dx}{r} \right)}$$

(14)

where $E[\Phi]$ is given by Equation (4), and $E[X = 0]$ is given by Equation (8). $|\Omega| = L^2$ is the area of the FoI.

Proof: From Equations (12)(13), the number of sensors required to achieving an expected occlusion coverage ratio is calculated by $n = \frac{ln(1-E[\mathcal{T}])}{ln \left(1 - \frac{E[\Phi]}{|\Omega|} \frac{\theta}{2\pi} \frac{\int_0^r e^{\sum_{i=1}^u \mu_i \left(\pi \overline{d_i}^2 + 2\overline{d_i}x \right)} dx}{r} \right)}$. The critical sensor density is the minimum number of sensors per
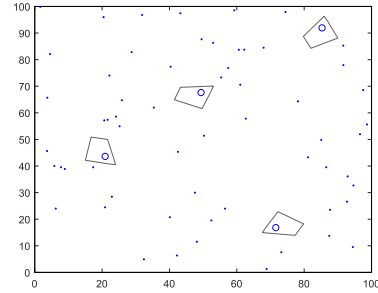

FIGURE 11. Illustration of system model in example 1. Four obstacles and 60 targets are located in the FoI.

unit area of the FoI, *i.e.*, $\rho = \frac{n}{|\Omega|}$ which the **Theorem 1** is proved.

Besides, the **Theorem 1** can be used to estimate the critical sensor density in traditional WSNs deployed in the FoI with irregular shape obstacles existence, at this time, the FoV angle of sensor $\theta = 2\pi$ substituting into Equation (14), we get the CSD model on occlusion coverage of partial target in WSNs.

Example 1: Given an square FoI with length of $100m$ as illustrated in Fig.11, in which 60 number of targets and some homogeneous sensors with $r = 15m$ and $\theta = \frac{\pi}{2}$ are scattered at random, respectively. In addition, four obstacles in group g_1 are randomly and uniformly located inside the FoI. In this case, the area of the 2D projection convex of each obstacle is set to $63.2864m^2$. Obviously, the other relevant parameters are calculated as: $l_1 = 9.1445, w_1 = 8.9788$. Then, we want to calculate the CSD in the FoI that the occlusion coverage ratio of targets is $E[\mathcal{H}] = 90\%$ with a high probability. Using Equation (4)(8) we obtain $E[\Phi] \approx 630.3583 \ m^2$, $E[X = 0] \approx 0.0.9326$. Substituting these parameters into Equation (14) in **Theorem 1**, we get $\rho \approx 0.0153$ and $n \approx 153$. That is, if we deploy 153 sensors in the FoI, we can ensure that 90% of targets are occlusion covered with a high probability.

VI. ANALYSIS OF NUMERICAL RESULTS

In this section, we take analysis of the numerical results of the expression derived in this paper. First, we take analysis of the influence of sensor density, sensing radius and FoV angle on the expected occlusion coverage ratio. Besides, we take the border effects into account and verified that the numerical results considering border effects have better performance than those without considering border effects.

For simplicity, we consider that the FoI is a square with length of $L = 100m$ as illustrated in Fig.12, in which 60 targets and homogeneous sensors are randomly scattered, respectively. Meanwhile, two groups (g_1 and g_2) of obstacles, independent of each other, are located in the FoI at random, and their area are respectively set to $63.2863m^2$ and $21.7653m^2$. The number of obstacles in g_1 and g_2 are fixed and equal, $\varpi_1 = \varpi_2 = 4$.

In order to get more accurate simulation results, we conduct each experiment $m = 100$ times to calculate the mean result representing the final simulation result. Besides, to better analyze the accuracy of the numerical results,
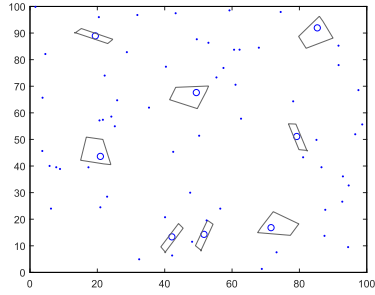
FIGURE 12. Illustration of system model in out simulation. Four g_1 and Four g_2 obstacles and 60 targets are located in the square FoI.
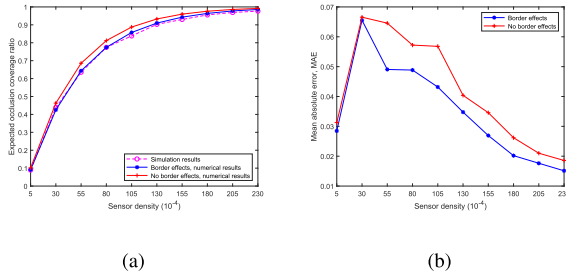

(a)   (b)

FIGURE 13. Impact of sensor densities on occlusion coverage ratio of targets, (a) Expected occlusion coverage ratio, (b) Mean absolute error.

(a)   (b)

FIGURE 14. Impact of sensing radii on occlusion coverage ratio of targets, (a) Expected occlusion coverage ratio, (b) Mean absolute error.

(a)   (b)

FIGURE 15. Impact of Fov angles on occlusion coverage ratio of targets, (a) Expected occlusion coverage ratio, (b) Mean absolute error.

we propose mean absolute error (MAE) expressed as

$$MAE = \frac{\sum_{i=1}^{m} |C_i - E[\mathcal{T}]|}{m} \qquad (15)$$

where C_i denote the ith simulation result of a experiment, and $E[\mathcal{T}]$ is the numerical result calculated by Equation (13).

A. IMPACT OF SENSOR DENSITY
Fig.13(a) and Fig.13(b) report the results of the expected occlusion coverage ratio and MAE under different sensor density. The results in the two figures are obtained in the case where sensing radius $r = 15m$ and FoV angle $\theta = \frac{2\pi}{3}$. Fig.13(a) indicates that the expected occlusion coverage ratio increases as the sensor density increases. Clearly, it can be seen that the numerical results approximately match the simulation results. The results show that the expected occlusion coverage ratio with no border effects almost exceeds that obtained by Equation (13), due to the PSR under no border effects is considered fully available for coverage contribution. An interesting observation is that for lower or higher sensor densities, the border efforts are not prominent, due to the expected occlusion coverage ratio approaches to 0 or 1. Moreover, From Fig.13(a), it is observed that the MAE is not greater than 0.07 under different sensor densities, and the MAE under border effects is almost less than that under no border effects.

B. IMPACT OF SENSING RADIUS
Here, we continue to analyze the influence of the sensing radii on the expected occlusion coverage ration under a fixed sensor density $\rho = 150 \times 10^{-4}$ and a fixed FoV angle $\theta = \frac{2\pi}{3}$. Fig.14(a) illustrates trend of expected occlusion coverage ratio under different sensing radii. Similar to the
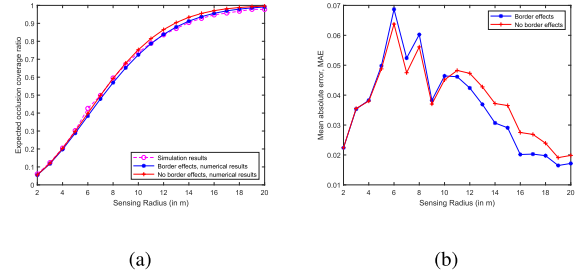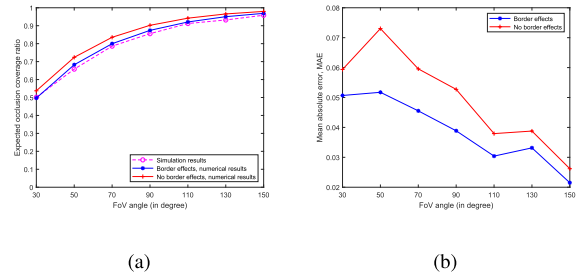
results in the previous section, it can be observed that the expected occlusion coverage ratio increases as the sensing radius increases, and the border effects are not significant for lower or higher sensing radii. When the sensing radii are in the range [7, 17], the border effects are prominent due to the more EPSR of a sensor close to the border will fall outside of the FoI. Fig.14(a) also shows that the numerical results obtained by Equation (13) have better fitting than those under no border effects. Meanwhile, Fig.14(b) shows that the MAE results are also controlled less than 0.07. When the border effects is not taken into account, the MAE results are almost greater than those under border effects.

C. IMPACT OF FoV ANGLE
Next, we study the influence of the FoV angles on the expected occlusion coverage ratio under a fixed sensor density $\rho = 150 \times 10^{-4}$ and a fixed sensing radius $r = 15m$. Fig.15(a) and 15(a) illustrate the trend like previous sections. It is easily concluded that the numerical results under border effects have better fitting than those under no border effects, and the MAE results have always been smaller and are controlled less than 0.052.

VII. CONCLUSION
This paper studied the target coverage problem in DSN with considering irregular shape obstacles existence. We defined the concept of occlusion coverage of partial targets and proposed the 2D projection model of a 3D obstacle. Furthermore, we introduced the expected occlusion zone to estimate the probability of none of obstacles occluding target. Then, we derived the critical sensor density for an expected occlusion coverage ratio of partial targets considering border effects, which has better accuracy compared with that

under no border efforts. In the end, a series of simulation experiments are carried out to verify the simulation results and numerical results. The research of this work would motivate further research on target coverage problem in DSN, such as targets coverage in rechargeable IoT networks with irregular obstacles existence.

REFERENCES

[1] N. Tekin, H. E. Erdem, and V. C. Gungor, "Analyzing lifetime of energy harvesting wireless multimedia sensor nodes in industrial environments," *Comput. Standards Interfaces*, vol. 58, pp. 109–117, May 2018.

[2] X. Yang, L. Shu, J. Chen, M. A. Ferrag, J. Wu, E. Nurellari, and K. Huang, "A survey on smart agriculture: Development modes, technologies, and security and privacy challenges," *IEEE/CAA J. Autom. Sinica*, vol. 8, no. 2, pp. 273–302, Feb. 2021.

[3] M. Naeem, W. Ejaz, M. Iqbal, F. Iqbal, A. Anpalagan, and J. J. P. C. Rodrigues, "Efficient scheduling of video camera sensor networks for IoT systems in smart cities," *Trans. Emerg. Telecommun. Technol.*, vol. 31, no. 5, May 2020, Art. no. e3798.

[4] V. Dyo, S. A. Ellwood, D. W. Macdonald, A. Markham, N. Trigoni, R. Wohlers, C. Mascolo, B. Pásztor, S. Scellato, and K. Yousef, "WILD-SENSING: Design and deployment of a sustainable sensor network for wildlife monitoring," *ACM Trans. Sensor Netw.*, vol. 8, no. 4, pp. 1–33, Sep. 2012.

[5] Z. Chen, H. Gao, Z. Zhang, H. Zhou, X. Wang, and Y. Tian, "Underwater salient object detection by combining 2D and 3D visual features," *Neurocomputing*, vol. 391, pp. 249–259, May 2020.

[6] H. M. Ammari and S. K. Das, "Critical density for coverage and connectivity in three-dimensional wireless sensor networks using continuum percolation," *IEEE Trans. Parallel Distrib. Syst.*, vol. 20, no. 6, pp. 872–885, Jun. 2009.

[7] H. P. Gupta, S. V. Rao, and T. Venkatesh, "Critical sensor density for partial coverage under border effects in wireless sensor networks," *IEEE Trans. Wireless Commun.*, vol. 13, no. 5, pp. 2374–2382, May 2014.

[8] B. Wang, J. Zhu, L. T. Yang, and Y. Mo, "Sensor density for confident information coverage in randomly deployed sensor networks," *IEEE Trans. Wireless Commun.*, vol. 15, no. 5, pp. 3238–3250, May 2016.

[9] Y. Yoon and Y.-H. Kim, "Maximizing the coverage of sensor deployments using a memetic algorithm and fast coverage estimation," *IEEE Trans. Cybern.*, vol. 52, no. 7, pp. 6531–6542, Jul. 2022.

[10] H. P. Gupta, S. V. Rao, and T. Venkatesh, "Critical sensor density for fault-tolerant coverage in 3D heterogeneous wireless sensor networks," in *Proc. IEEE Int. Conf. Adv. Netw. Telecommun. Syst. (ANTS)*, Kattankulathur, India, Dec. 2013, pp. 1–6.

[11] D. Saha, S. Pal, N. Das, and B. B. Bhattacharya, "Fast estimation of area-coverage for wireless sensor networks based on digital geometry," *IEEE Trans. Multi-Scale Comput. Syst.*, vol. 3, no. 3, pp. 166–180, Jul. 2017.

[12] M. Karakaya and H. Qi, "Coverage estimation for crowded targets in visual sensor networks," *ACM Trans. Sensor Netw.*, vol. 8, no. 3, pp. 1–22, Jul. 2012.

[13] M. Khanjary, M. Sabaei, and M. R. Meybodi, "Critical density for coverage and connectivity in two-dimensional aligned-orientation directional sensor networks using continuum percolation," *IEEE Sensors J.*, vol. 14, no. 8, pp. 2856–2863, Aug. 2014.

[14] M. Khanjary, M. Sabaei, and M. R. Meybodi, "Critical density in adjustable-orientation directional sensor networks using continuum percolation," *Proc. Comput. Sci.*, vol. 116, pp. 548–555, Dec. 1017.

[15] A. M. Attar, S. Yarahmadian, and S. Samavi, "Coverage estimation in heterogenous floorplan visual sensor networks," in *Proc. IEEE Sensors*, Baltimore, MD, USA, Nov. 2013, pp. 1–4.

[16] Y. Wang and G. Cao, "On full-view coverage in camera sensor networks," in *Proc. IEEE INFOCOM*, Apr. 2011, pp. 1781–1789.

[17] Y. Wang and G. Cao, "Achieving full-view coverage in camera sensor networks," *ACM Trans. Sensor Netw.*, vol. 10, no. 1, pp. 1–31, Nov. 2013.

[18] X. Gan, Z. Zhang, L. Fu, X. Wu, and X. Wang, "Unraveling impact of critical sensing range on mobile camera sensor networks," *IEEE Trans. Mobile Comput.*, vol. 19, no. 4, pp. 982–996, Apr. 2020.

[19] Z. Liu and G. Jiang, "Sensor parameter estimation for full-view coverage of camera sensor networks based on bounded convex region deployment," *IEEE Access*, vol. 9, pp. 97129–97137, 2021.

[20] Z. Yu, F. Yang, J. Teng, A. C. Champion, and D. Xuan, "Local face-view barrier coverage in camera sensor networks," in *Proc. IEEE Conf. Comput. Commun. (INFOCOM)*, Hong Kong, Apr. 2015, pp. 684–692.

[21] L. Kang, Y. Qi, W. Gao, A. Wang, and Z. Dong, "A percolation based approach for critical density in non-orientation directional sensor network," in *Proc. IEEE Int. Conf. Ubiquitous Comput. Commun. (IUCC), Data Sci. Comput. Intell. (DSCI), Smart Comput., Netw. Services (SmartCNS)*, Oct. 2019, pp. 89–94.

[22] J.-M. Lien and N. M. Amato, "Approximate convex decomposition of polyhedra," in *Proc. ACM SIGGRAPH Posters (SIGGRAPH)*, 2004, pp. 121–131.

[23] J. R. Kala, S. Viriri, and J. R. Tapamo, "An approximation based algorithm for minimum bounding rectangle computation," in *Proc. IEEE 6th Int. Conf. Adapt. Sci. Technol. (ICAST)*, Ota, Nigeria, Oct. 2014, pp. 1–6.

ZHIMIN LIU was born in Chenzhou, China. He received the B.E. degree from Northeastern University, in 2006, the M.E. degree from South China Agricultural University, in 2010, and the Ph.D. degree from Central South University, in 2017. He is currently a Lecturer with the School of Mathematics and Computational Science, Hunan First Normal University. His current interests include wireless camera sensor networks, sensor clouds, and crowd sensing.

ZUOQING CAO was born in Chenzhou, China. He received the B.E. degree from Central South University, in 2007. Currently, he is a Lecturer with the School of Mapping and Geography, Hunan Engineering Vocational and Technical College. His current research interests include wireless camera sensor networks, sensor clouds, and unmanned aerial vehicles.
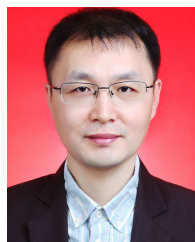
SHUKUN LIU (Member, IEEE) was born in Cangzhou, Hebei, China. He received the Ph.D. degree in computer science and technology from Central South University, Changsha, China, in 2016. From 2013 to 2019, he was an associate professor. Since 2020, he has been a Professor of computer science and technology with Hunan Women's University. His current research interests include cloud computing, computer networks, virtualization technology, database technology, data mining, and software engineering. He has published more than 30 technical articles and books in the above areas. His research is supported by the Hunan Provincial Natural Science Foundation and the Hunan Provincial Education Department Scientific Research Foundation. He is a member of CCF.

PINIAL KHAN BUTT received the master's degree in telecommunication technology from the University of Sindh, Pakistan, in 2002, and the Ph.D. degree in computer science and technology from the School of Information Science and Engineering, Central South University, Changsha, Hunan, China, in 2017. He is currently a Professor with the Information Technology Center, Sindh Agricultural University, Tando Jam, Pakistan. His current research interests include e-commerce telecommunication technology and energy-efficient mobile computing.

● ● ●